

IRSTI 29.03.77

<sup>1</sup>F.F. Komarov, <sup>2\*</sup>T.A. Shmygaleva, <sup>2</sup>N. Akanbay, <sup>2</sup>S.A. Shafii, <sup>3</sup>A.A. Kuatbayeva

<sup>1</sup>Belarusian state university, Minsk, Belarus

<sup>2</sup>al-Farabi Kazakh National university, Almaty, Kazakhstan

<sup>3</sup>Sh.Ualikhanov Kokshetau State university, Kokshetau, Kazakhstan

\*e-mail: shmyg1953@mail.ru

### **Optimization calculation algorithms on cascade and probabilistic functions and radiation defects concentration at the ionic radiation**

**Abstract.** Work is performed within a cascade and probabilistic method which essence consists in receiving and further usage of the cascade and probabilistic functions (CPF) for various particles. CPF make sense to probability that the particle generated at some depth of  $h'$  will reach a certain depth of  $h$  after  $n$  number of impacts. In work optimization calculation algorithms of the cascade and probabilistic functions (CPF) depending on interactions number and particles penetration depth is offered, concentration of radiation defects at ionic radiation for the purpose of reduction calculation time and quality. For calculation CPF and concentration radiation defects there is an area of result, border of this area and a calculation step. Borders and a calculation step selection automation is executed.

**Key words:** Optimization, algorithm, calculation, cascade and probabilistic, ion, defect formation, binary search, ternary search, function.

#### **Introduction**

In recent years much attention is paid to questions of various processes mathematical modeling. Mathematical models development, calculation algorithms, research objects allows to describe many phenomena [1-3]. Modeling on the computer radiation defect formation processes in solid bodies at radiation is considered by us their various charged particles and computer modeling features on cascade and probabilistic functions and radiation defects for ions. Such works necessity is connected with a solid body defects generation and evolution management problem, for receiving, eventually, materials with the set properties [4]. For metals radiation by ions is in an efficient manner changes of such properties as the metal durability, corrosion resistance, fatigue, depreciation etc. In this direction the solid body radiation physics would be left rather academic occupation which isn't interest to practical applications without researches. It is necessary to notice that a large number of works is devoted to radiation defect formation at interaction

of ions with substance problems, for example [5-8]. Losses of energy on ionization and electron shells excitement of the environment atoms weren't considered, therefore the elementary CPF was used. At charged particles to substance interaction on their movement way there are continuous energy losses. These losses result in strong dependence for both power the flying particles spectrum, and the primary beaten-out atoms (PBOA) from penetration depth. The interaction run on PBOA formation significantly depends on energy in this connection there was a need of receiving the physical and mathematical models considering real dependences of the elementary act various parameters on energy, depth.

Earlier in most cases at concrete calculations the elementary cascade and probabilistic function (CPF) was generally used, it isn't always justified as the run of interaction depends on energy [9,10]. It is necessary to investigate the received CPF behavior taking into account energy losses for ions, prove properties which they have to possess both with physical, and with mathematical points of view,

develop calculations algorithms and make CPF calculations depending on interactions number and particles penetration depth, spectrums of primary beaten-out atoms and radiation defects concentration.

Nowadays well-known methods are next: the Monte Carlo method, the Boltzmann kinetic equation, Fokker-Planck's equation, Lindhard's methods, Vineyard's methods, etc. The choice of this or that method applicability is very complex challenge as, on the one hand, because of similar tasks complexity often it is necessary to apply too many approximations which significantly worsen the calculations accuracy to obtaining final result, and on the other hand – for obtaining qualitative result it is necessary to overcome very great computing difficulties. Eventually, everything is defined by a problem specifics and the researcher ability to apply this or that method to the specific objective solution. The cascade and probabilistic method is one of options in theoretical methods numerous calculation for the spatial and power distributions of the falling and secondary particles in the environment [9–11]. From this point of view it's usage in scientific research is necessary.

### Main results

The following physical model is given. Charged particle on the movement way continuously loses the energy on ionization and excitement (energy

losses for each particles grade depending on energy are known and described by analytical expressions, in particular, by the Bethe-Bloch formula) [10]. Impacts happen to atoms, cores discretely. After crashes primary particles keep the movement direction. At the movement charged particles through substance their run depends on energy through the interaction section which is calculated for ions by Rutherford's formula [10]. Observations depths are according to the tables of the ion-implanted impurity spatial distribution parameters [12]. The calculated interaction section is approximated by the following expression:

$$\lambda(h) = \frac{1}{\lambda_0} \left( \frac{1}{a(E_0 - kh)} - 1 \right), \quad (1)$$

$\lambda_0, a, E_0, k$  – approximation parameters,  $\sigma_0 = 1/\lambda_0$ .

From a recurrence relation for transition probabilities

$$\psi_n(h', h, E_0) = \int_{h'}^h \psi_{n-1}(h', h'', E_0) \psi_0(h'', h, E_0) \frac{1}{\lambda_0} \left( \frac{1}{a(E_0 - kh'')} - 1 \right) dh'', \quad (2)$$

we receive expression for CPF taking into account energy losses for ions in the following look:

$$\psi_n(h', h, E_0) = \frac{1}{n! \lambda_0^n} \left( \frac{E_0 - kh'}{E_0 - kh} \right)^{-l} \exp \left( \frac{h - h'}{\lambda_0} \right) * \left[ \frac{\ln \left( \frac{E_0 - kh'}{E_0 - kh} \right)}{ak} - (h - h') \right]^n, \quad (3)$$

where  $n$  – interactions number,  $h', h$  – ion generation and registration depths,  $l = 1/(\lambda_0 ak)$ .

Calculations of cascade and probabilistic

functions taking into account energy losses for ions depending on interactions number and particles penetration depth were carried out on a formula:

$$\psi_n(h', h, E_0) = \prod_{i=1}^n \left( \frac{\ln \left( \frac{E_0 - kh'}{E_0 - kh} \right)}{ak} - (h - h') \right) \frac{1}{\lambda_0^i} * \exp \left( \left( \frac{h - h'}{\lambda_0} \right) - \frac{1}{\lambda_0 ak} \ln \left( \frac{E_0 - kh'}{E_0 - kh} \right) \right). \quad (4)$$

For optimization CPF calculation algorithms depending on interactions number and particles penetration depth, vacancy clusters concentration are used Stirling formulas [13]:

$$n! \approx n^n e^{-n} \sqrt{2\pi n}. \tag{5}$$

$$\ln n! \approx \left(n + \frac{1}{2}\right) \ln n - n + \frac{1}{2} \ln(2\pi). \tag{6}$$

Ions spend the main energy part for ionization and excitement the environment atoms (to 99%) and only 1% goes for atomic structure defects formation. At charged particles with material interaction dot defects, Frenkel's couples, big congestions the vacancy and interstitial atoms can be formed.

Radiation defects at ionic radiation concentration calculation is carried out on a formula [11]:

$$C_k(E_0, h) = \int_{E_c}^{E_{2max}} W(E_0, E_2, h) dE_2, \tag{7}$$

$$E_{2max} = \frac{4m_1c^2 m_2c^2}{(m_1c^2 + m_2c^2)^2} E_1;$$

$E_{2max}$  – the greatest possible energy acquired by atom,  $m_1c^2$  – an ion rest energy.  $C_k(E_0, h)$  is defined taking into account that a particle energy at  $h$  depth is  $E_1(h)$ . As  $E_1(h) = E_0 - \Delta E(h)$ , that setting energy losses on ionization and excitement  $\Delta E(h)$ , we receive the corresponding observations  $h$  depths from a Bethe-Bloch formula. The primary beaten-out atoms spectrum is defined by the following ratio:

$$W(E_0, E_2, h) = \sum_{n=n_0}^{n_1} \int_{h-k\lambda_2}^h \psi_n(h') \exp\left(-\frac{h-h'}{\lambda_2}\right) \frac{w(E_1, E_2, h') dh'}{\lambda_1(h') \lambda_2}, \tag{8}$$

where  $n_0, n_1$  – initial and final value of interactions number from a cascade and probabilistic function

definition range. CPF  $\psi_n(h')$ , entering expression (8), has next appearance:

$$\psi_n(h') = \frac{1}{n! \lambda_0^n} \left(\frac{E_0}{E_0 - kh'}\right)^{\frac{1}{\lambda_0 ak}} \exp\left(\frac{h'}{\lambda_0}\right) \left(\frac{\ln\left(\frac{E_0}{E_0 - kh'}\right)}{ak} - h'\right)^n, \tag{9}$$

$$\lambda_1(h') = \frac{1}{\sigma_0 n_0 \left(\frac{1}{a(E_0 - kh')} - 1\right)} * 10^{24} \text{ (cm)}, \quad \lambda_2 = \frac{1}{\sigma_2 n_0} * 10^{24} \text{ (cm)}.$$

Section  $\sigma_2$  is calculated by Rutherford's formula,  $\lambda_1, \lambda_2$  – run on an ion - atomic and atom - atomic impact respectively;  $k$  – integer bigger units;  $w(E_1, E_2, h')$  – PBOA spectrum in the elementary act,  $E_2$  – primary beaten-out atom energy.

The PBOA spectrum in the elementary act is calculated on a formula:

$$\omega(E_1, E_2) = \frac{d\sigma(E_1, E_2) / dE_2}{\sigma(E_1)}. \tag{10}$$

Substituting expression (10) in formulas (7), (8) we receive:

$$C_k(E_0, h) = \frac{E_d E_{2max}}{E_{2max} - E_d} \int_{E_c}^{E_{2max}} \frac{dE_2}{E_2^2} \sum_{n=n_0}^{n_1} \int_{h-k\lambda_2}^h \psi_n(h') \exp\left(-\frac{h-h'}{\lambda_2}\right) \frac{dh'}{\lambda_1(h') \lambda_2}$$

Carrying out transformations, we come to the following expression:

$$C_k(E_0, h) = \frac{E_d (E_{2\max} - E_c)}{E_c (E_{2\max} - E_d)} \sum_{n=n_0}^{n_1} \int_{h-k\lambda_2}^h \psi_n(h') \exp\left(-\frac{h-h'}{\lambda_2}\right) \frac{dh'}{\lambda_1(h')\lambda_2}, \quad (11)$$

where  $E_d$  – average energy of shift,  $E_0$  – initial energy of a particle,  $E_c$  – threshold energy.

To calculate radiation defects concentration on a

formula (11) with usage (9) it is impossible as in each member of CPF there is an overflow.

Expression for  $\psi_n(h')$  it is presented in the form:

$$\Psi_n(h', h, E_0) = \exp\left(-\ln n! - n \ln \lambda_0 - \frac{1}{\lambda_0 a k} \ln\left(\frac{E_0}{E_0 - kh'}\right) + \frac{h'}{\lambda_0} + n \ln\left(\frac{\ln\left(\frac{E_0}{E_0 - kh'}\right)}{a k} - h'\right)\right). \quad (12)$$

When calculating CPF for ions there are difficulties consisting in approximating coefficients selection and in finding real area of result both depending on interactions number and from penetration depth. The area of result is influenced by the flying particle and target atomic number, initial

energy of primary particle and penetration depth. All CPF calculations for a formula (4) have been made on a C#, as the DBMS for dataful operation MS SQL Server 2014 environment was used. CPF calculations results for ions depending on interactions number and particles penetration depth are given in figures 1,2.

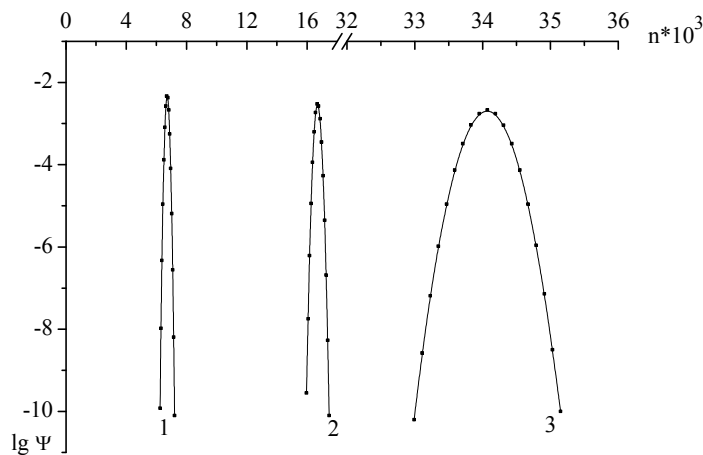


**Figure 1** – CPF dependence on interactions number for the titan in iron at  $h=0,0001; 0,0002; 0,0003$  (cm);  $E=1000$  keV (1-3)

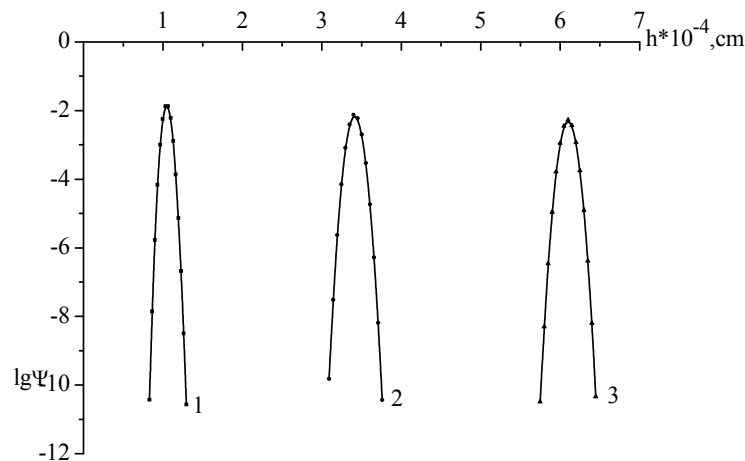


**Figure 2** – Dependency  $\psi_n(h', h, E_0)$ , from  $h$  for aluminum in the titan at  $E_0 = 800$  keV for  $n = 732; 2702; 5697$  (1-3)

Due carrying out CPF calculations depending on impacts number and particles penetration depth of result area behavior and a calculation step regularities are revealed. Let's note some of them. Result area behavior regularities for CPF calculated depending on interactions number consist in the following:

1. With initial energy (the flying particle and a target same) reduction with the same depth the area of result is narrowed and displaced to the left.

2. With the flying particle increase in atomic weight the area of result finding is displaced to the left relatively  $h/\lambda$  and is narrowed.

3. With the flying particle big atomic weight the CPF maximum value is displaced to the left relatively  $h/\lambda$  already with small depths, and with big depths the result is in narrow area.

4. The narrowest area of result turns out with the flying particle big atomic weight and small target on the end of a run.

At the step choice following regularities take place:

1. For the flying particle small atomic weight and small depths the step is small (about 10-20), with increase in observation depth it begins to increase.

2. With the flying particle atomic weight gain in the step respectively increases, reaching several hundred and even thousands.

3. With the flying particle big atomic weight and small targets the step considerably increases.

Let's give the regularities arising due finding a real range defined for CPF calculated depending on penetration depth:

1. Calculations shows that a small atomic weight of the flying particle and small depths area of result CPF depending on  $h$  is close to  $h$ , which corresponds  $h/\lambda$ . With increase in observation depth the area of result is displaced to the right and narrowed.

2. With initial energy of a particle (the flying particle and a target same) reduction with the same observation depth the area of result is displaced to the right and narrowed.

3. With increase observation in depth for any flying particle and any target the area of result is displaced to the right.

4. Depending on the flying particle atomic number at the same value of depth  $h$  the area of result is displaced to the right.

5. At the flying particle atomic number great value the area of result is displaced to the right relatively  $h$ , corresponding  $h/\lambda$  already with small depths and the area of result is considerably narrowed.

Step behavior regularities due CPF calculating depending on particles penetration depth are revealed.

1. For the flying particle small atomic weight the step is small, with increase in observation depth it increases, and on the end of a run very strongly.

2. With initial energy of a particle with the same observation depth (the flying particle and a target same) reduction the step also increases.

3. With the flying particle atomic weight increase for the same observation depth the step increases at first gradually, then is very sharp.

4. Step on atomic number dependence tends increase.

For automation and optimization finding CPF area of result depending on interactions number, penetration depths have been realized algorithms Ternary [14] and Binary [15] searches. The Ternary search algorithm has been modified taking into account CPF specifics: it exists in limited area. In the existing algorithms the division coefficient equal to 3 is used (ternary search). In the developed program complex the coefficient can vary. Binary (binary) search (it is also known as a halving and a dichotomy method) - the classical element search algorithm in the sorted array (vector) uses array crushing on half. It is used in computer science, calculus mathematics and mathematical programming. Ternary search is a method in computer science for finding the minimum or maximum of function, which at first strictly increases, then strictly decreases, or on the contrary.

Ternary search defines that the minimum or a maximum can't lie either in the first, or in the last third of area, and then repeats search on the remained two thirds.

The concentration values calculated by a formula (11) have the following behavior: for the easy flying particles curves increase, reaching a maximum, then decreases to zero. With initial energy of a particle increase curves are displaced to the right. With increase in threshold energy  $E_c$  concentration values decreases and curves pass much below, transition through a maximum is carried out more smoothly. While energy  $E_0 = 100$  keV the curve decreases. Due the flying particle increase in atomic weight the value of function in a maximum point increases and, therefore, curves pass above while values of depths decrease. Calculation algorithms optimization with formulas (5), (6) usage is performed. After carrying out optimization in formulas (4), (11) it is visible what a counting duration was considerably reduced, for example, for germanium in aluminum at  $E_0 = 1000$  keV,  $E_1 = 120$  keV calculation time was 1 hour 44 minutes. After optimization calculation time has less than 1 minute. Calculations comparison results before optimization and after it is given in the table 1.

**Table 1** – Definition range borders of radiation defects concentration for germanium in silicon at  $E_c = 50$  keV и  $E_0 = 1000$  keV

$h \cdot 10^4$ , cm	$C_k$ , cm	$E_0$ , keV	$n_0$	$n_1$	$\tau_1$	$\tau_2$
0,1	10476	1000	219	560	5'	1"
5,3	17598	800	25146	27958	10'	2"
10,6	29380	600	69624	74258	25'	3"
15,8	51189	400	147578	154312	1h	7"
18,9	77629	300	227841	236220	3h29'	15"
19,9	90354	260	264188	273220	4h12'	20"
20,9	107041	220	308961	318741	5h30'	25"
21,8	124137	180	359803	368257	7h06'	35"
22,3	123290	140	394307	403204	10h01'	1'
23,2	118373	100	474116	486299	12h41'	2'
23,9	50357	70	563193	575375	15h26'	7'
24,1	-20064	60	596160	608342	17h19'	10'

Here  $\tau_1$ ,  $\tau_2$  – calculation time before carrying out optimization and after it.

Calculations results of are given in figures 3-5 and in tables 2-5 [16-21].

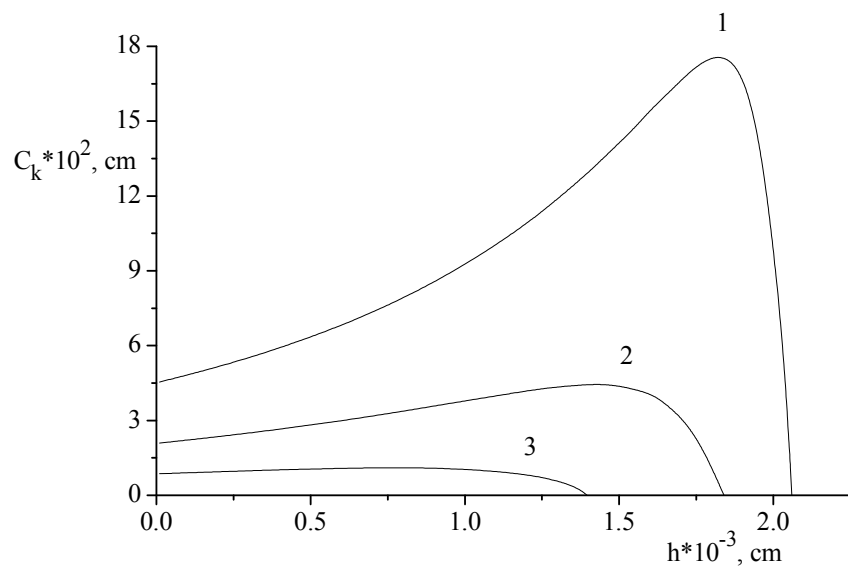


**Figure 3** – Radiation defects concentration dependence on depth for the titan nitrogen ions radiation at  $E_0=1000$  keV,  $E_c=50$  keV(1), 100 keV (2), 200 keV (3)

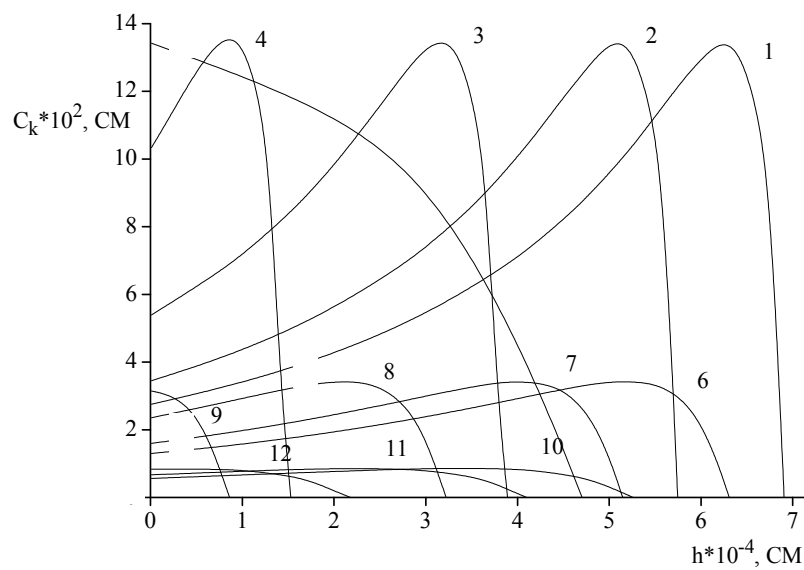


**Figure 4** – Radiation defects concentration dependence on depth in the ionic radiation for nitrogen in silicon at  $E_c=50$  keV;  $E_0= 1000, 800, 500, 200, 100$  keV (1-5);  $E_c=100$  keV;  $E_0= 1000, 800, 500, 200$  keV (6-9);  $E_c=200$  keV;  $E_0= 1000, 800, 500$  keV (10-12)

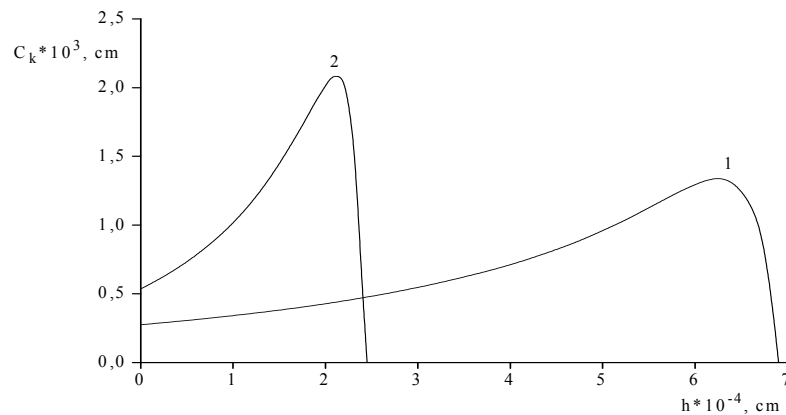


**Figure 5** – Radiation defects concentration dependence on depth in the ionic radiation for nitrogen in silicon (1) and nitrogen in germanium (2) at  $E_0=1000$  keV;  $E_c=50$  keV

Finding the radiation defects concentration area of result at ionic radiation has allowed to find this area's behavior regularities. Let's note some of them.

1. With increase in threshold energy with the same penetration depth value of radiation defects concentration considerably decreases, area of result borders don't change.

2. Depending on penetration depth the radiation defects concentration value increases.

3. With increase in primary particle initial energy at the same value of threshold energy and penetration depth, value of radiation defects concentration decreases.

4. The radiation defects concentration area of result borders depending on penetration depth increases, the borders change range fluctuates from 0 to 5000.

5. Depending on threshold energy at the same energy and the same penetration depth the border don't change.

**Table 2** – Radiation defects concentration definition range borders for nitrogen in the titan at  $E_c=50$  keV,  $E_0=1000$  keV

$h \cdot 10^4, \text{ cm}$	$C_k, \text{ cm}$	$E_0, \text{ keV}$	$n_0$	$n_1$	$\tau$
0,1	453,93	1000	0	27	1"
1,7	504,21	900	61	224	3"
3,5	569,57	800	196	439	4"60
5,4	650,76	700	376	681	6"
7,3	747,10	600	596	970	7"90
9,4	878,12	500	894	1341	9"
11,6	1050,64	400	1286	1840	13"
12,8	1165,35	350	1545	2142	14"
14	1294,26	300	1846	2474	15"70
14,5	1352,72	280	1987	2648	17"
15	1412,73	260	2138	2820	18"
15,5	1473,16	240	2301	2995	19"
16,1	1556,9	220	2514	3247	21"
16,6	1612,65	200	2709	3461	22"
17,2	1688,03	180	2967	3795	24"50
17,8	1746,76	160	3258	4105	26"
18,4	1765,86	140	3588	4455	29"
19	1695,9	120	3971	4885	31"45
19,6	1422,67	100	4422	5397	35"
20,3	677,95	80	5071	6110	41"
20,6	0	70	5406	6452	42"

**Table 3** – Radiation defects concentration definition range borders for nitrogen in the aluminum at  $E_c=50$  keV и  $E_0=1000$  keV

$h \cdot 10^4$ , cm	$C_k$ , cm	$E_0$ , keV	$n_0$	$n_1$
0,1	296	1000	0	32
3,5	335	900	84	310
7,1	381,5	800	250	583
10,9	439	700	469	899
14,9	511	600	751	1277
19,1	605	500	1116	1742
23,6	734	400	1607	2344
26	817	350	1923	2723
28,5	919	300	2304	3175
29,6	970	280	2493	3396
30,6	1017,6	260	2677	3611
31,7	1074	240	2895	3864
32,9	1142	220	3154	4163
34	1205	200	3414	4463
35,2	1278	180	3728	4821
36,5	1361	160	4108	5253
37,7	1422	140	4505	5703
39,1	1487,2	120	5041	6300
40,4	1460	100	5630	6965
41,9	1270	80	6465	7894
42,6	976	70	6934	8414
43,4	413	60	7558	9102
44,1	-745	50	8207	9816

**Table 4** – Radiation defects concentration definition range borders for nitrogen in the silicon at  $E_c=200$  keV и  $E_0= 800$  keV

$h \cdot 10^4$ , cm	$C_k$ , cm	$E_0$ , keV	$n_0$	$n_1$	$\tau$
0,1	66,71	800	0	32	01"15
6,1	73,10	700	598	972	02"30
12,5	79,67	600	1499	2060	05"42
19,3	85,05	500	2688	3428	10"49
26,5	84,91	400	4271	5228	46"56
30,3	79,16	350	5282	6307	1' 01"10
34,2	64,25	300	6483	7634	1' 17"50
35,9	54,08	280	7070	8249	1' 24"09
37,6	39,79	260	7701	8926	1' 31"41
39,3	19,77	240	8384	9700	1' 44"40
41,0	0	220	9124	10461	1' 52"80

**Table 5** – Radiation defects concentration definition range borders for carbon in the titan at  $E_c=100$  keV,  $E_0= 500$  keV

$h \cdot 10^4$ , cm	$C_k$ , cm	$E_0$ , keV	$n_0$	$n_1$	$\tau$
0,1	213,66	500	0	30	1"
2,1	238,34	400	132	337	4"
3,3	251,38	350	269	541	7"
4,5	255,62	300	439	769	9"
5	253,24	280	520	881	13"
5,5	246,35	260	610	994	17"
6	232,94	240	705	1110	24"
6,5	210,03	220	811	1252	26"

7,1	176,16	200	951	1423	33"
7,7	119,25	180	1109	1610	36"
8,2	24,45	160	1256	1789	11"
8,8	0	140	1456	2044	12"

## Conclusions

In work, analytical expressions of cascade and probabilistic functions taking into account energy losses for ions from recurrence relations for transition probabilities are received. The approximating expression entering a recurrence relation is picked up and approximation coefficients are found, so that the theoretical correlation relation was rather high [22-24]. Algorithms are developed and optimization of calculation cascade and probabilistic functions taking into account energy losses depending on interactions number and particles penetration depth, radiation defects concentration is made at ionic radiation, calculations are carried out. Behavior regularities on CPF area of result and calculation step depending on interactions number and particles penetration depth are revealed. It is shown that the area of result is influenced significantly by the primary particle initial energy, penetration depth, the flying particle atomic number and target. Automation and optimization area of result borders selection and calculation step with ternary and binary search algorithms usage is executed. Algorithms optimization on calculation the cascade and probable functions taking into account energy losses, depending on interactions number and particles penetration depth, concentration the vacancy clusters is performed in the ionic radiation case with Stirling formula usage. Results comparison of calculation for time before carrying out optimization and after it is executed. The program complex is developed in the Microsoft Visual Studio 2015 environment in the C# programming language. The database is created in the Microsoft Server 2014 environment.

## References

1. E.G. Boos, A.A. Kupchishin, A.I. Kupchishin, E.V. Shmygalev, T.A. Shmygaleva. Cascade and probabilistic method, solution of radiation and physical tasks, Boltzmann's equations. Communication with Markov's chains. -Monograph. Almaty: KazNPU after Abay, Scientific Research Institute for New Chemical Technologies and Materials under al-Farabi KazNU, 2015. – 388 p.
2. Czarnaacka, K., Komarov, F.F., Romanov, I.A., Zukowski, P., Parkhomenko, I.N. AC measurements and dielectric properties of nitrogen-rich silicon nitride thin films. // Proceedings of the 2017 IEEE 7th International Conference on Nanomaterials: Applications and Properties, NAP 2017. - No. 5. P. 657-669.
3. Komarov, F.F., Milchanin, O.V., Parfimovich, I.D., Tkachev, A.G., Bychanok, D.S. Absorption and Reflectance Spectra of Microwave Radiation by an Epoxy Resin Composite with Multi-Walled Carbon Nanotubes. //Journal of Applied Spectroscopy.-2017. – Vol. 84. – No. 4. –P. 570-577.
4. Komarov F.F. Nano- and microstructuring of solids by swift heavy ions//Physics-Uspekhi. - 2017. – Vol. 187. – No. 5. –P. 465-504.
5. Komarov, F.F., Romanov, I.A., Vlasukova, L.A., Mudryi, A.V., Wendler, E. Optical and Structural Properties of Silicon with Ion-Beam Synthesized InSb Nanocrystals.// Spectroscopy.-2017. – Vol. 120. – No. 1. –P. 204-207.
6. Komarov, F.F., Konstantinov, S.V., Strel'nitskij, V.E., Pilko, V.V. Effect of Helium ion irradiation on the structure, the phase stability, and the microhardness of TiN, TiAlN, and TiAlYN nanostructured coatings. //Technical Physics.-2016. – Vol. 61. – No. 5. –P. 696-702.
7. Al'zhanova, A., Dauletbekova, A., Komarov, F., Akilbekov, A., Zdorovets, M. Peculiarities of latent track etching in SiO<sub>2</sub>/Si structures irradiated with Ar, Kr and Xe ions.-2016. – Vol. 374. – No. 1. –P. 121-124.// Nuclear Instruments and Methods in Physics Research, Section B: Beam Interactions with Materials and Atoms.-2016. – Vol. 426. – No. 1. –P. 1-56.
8. Komarov, F.F., Zayats, G.M., Komarov, A.F., Michailov, V.V., Komsta, H. Simulation of radiation effects in SiO<sub>2</sub>/Si Structures.// Acta Physica Polonica A.-2015. . – Vol. 3. – No. 1. –P. 854-860.
9. Komarov, F., Uglov, V., Vlasukova, L., Zlotski, S., Yuvchenko, V. Drastic structure changes in pre-damaged GaAs crystals irradiated with swift heavy ions.// Nuclear Instruments and Methods in Physics Research, Section B: Beam Interactions with Materials and Atoms.-2015. – Vol. 360. – No. 4. –P. 150-155.

10. Kodanova, S.K., Ramazanov, T.S., Issanova, M.K., Golyatina, R.I., Maierov, S.A Calculation of ion stopping in dense plasma by the Monte-Carlo method.// *Journal of Physics: Conference Series*.-2018. – Vol. 946. – No. 1. – P. 148-154.
11. Smyrnova, K.V., Pogrebnyak, A.D., Beresnev, V.M., Kravchenko, Y.O., Bondar, O.V. Microstructure and Physical–Mechanical Properties of (TiAlSiY)N Nanostructured Coatings Under Different Energy Conditions.// *Metals and Materials International*.-2018. – Vol. 24. – No. 2. –P. 241-439.
12. Kozhamkulov, B.A., Kupchishin, A.I., Bitibaeva, Z.M., Tamuzs, V.P. Radiation-Induced Defect Formation in Composite Materials and Their Destruction Under Electron Irradiation // *Mechanics of Composite Materials*. -2017. – Vol. 53. – No. 1. – P. 59-64.
13. Kupchishin, A.I. On positrons irradiation in the defects of vacancy type.// *IOP Conference Series: Materials Science and Engineering*.-2017. – Vol. 184. – No. 1. –P. 234-248.
14. Kupchishin, A.I., Niyazov, M.N., Voronova, N.A., Kirdiyashkin, V.I., Abdukhairova, A.T. The effect of temperature, static load and electron beam irradiation on the deformation of linear polymers.// *IOP Conference Series: Materials Science and Engineering*.-2017. – Vol. 168. – No. 1. –P. 229-274.
15. Kupchishin, A.I., Kupchishin, A.A., Voronova, N.A. Cascade-probabilistic methods and solution of Boltzman type of equations for particle flow// *IOP Conference Series: Materials Science and Engineering*. – 2016. Vol. 110. – No. 1. – P. 123-129.
16. Kupchishin, A.I., Kupchishin, A.A., Voronova, N.A., Kirdiyashkin, V.I. Positron sensing of distribution of defects in depth materials. // *IOP Conference Series: Materials Science and Engineering*. -2016. - Vol. 110. – No. 4. – P. 248-258.
17. Nowak, S.H., Bjeoumikhov, A., von Borany, J., Wedell, R., Ziegenrucker, R. Examples of XRF and PIXE imaging with few microns resolution using SLcam® a color X-ray camera // *X-Ray Spectrometry*. – 2015. – Vol. 44. – No. 3. – P. 135-140.
18. Bjeoumikhov, A., Buzanich, G., Langhoff, N., Soltau, H., (...), Wedell, R. The SLcam: A full-field energy dispersive X-ray camera.// *Journal of Instrumentation*.-2012. - Vol. 7. – No. 5. – P. 248-252.
19. Bock, M., Skibina, J., Fischer, D., (...), Beloglazov, V., Steinmeyer, G. Nanostructured fibers for sub-10 fs optical pulse delivery.// *Laser and Photonics Reviews*.- 2013. - Vol. 7. – No. 3. – P. 566-570.
20. Dubovichenko, S., Burtebayev, N., Dzhazairov-Kakhramanov, A., (...), Kliczewski, S., Sadykov, T. New measurements and phase shift analysis of p16O elastic scattering at astrophysical energies.// *Chinese Physics C*.-2017. - Vol. 41. – No. 1. –P. 485-495.
21. Kupchishin, A.I., Shmygalev, E.V., Shmygaleva, T.A., Jorabayev, A.B. Relationship between markov chains and radiation defect formation processes by ion irradiation.// *Modern Applied Science*.- 2015. – Vol. 9. – No. 3. – P. 59-70.
22. Kupchishin, A.I., Kupchishin, A.A., Shmygalev, E.V., Shmygaleva, T.A., Tlebaev, K.B. Calculation of the spatial distribution of defects and cascade- Probability functions in the materials.// *Journal of Physics: Conference Series*. – 2014. – Vol. 552. – No. 2. – P. 89-96.
23. Voronova N. A., Kupchishin, A.I., Kupchishin, A.A., Kuatbayeva A.A., Shmygaleva, T.A., "Computer Modeling of Depth Distribution of Vacancy Nanoclusters in Ion-Irradiated Materials".// *Key Engineering Materials*. – 2018. – Vol. 769. – P. 358-363.